HiLL PUBLISHING

Journal of Applied Mathematics and Computation, 2023, 7(2), 224-233
https://www.hillpublisher.com/journals/JAMC/
ISSN Online: 2576-0653
ISSN Print: 2576-0645

Mathematical Analysis of an SIR Model with Local and Global Infections Based on Trinomial Distribution

Mengke Ren

School of Mathematics and Physics, China University of Geosciences, Wuhan, Hubei, China.

How to cite this paper: Mengke Ren. (2023) Mathematical Analysis of an SIR Model with Local and Global Infections Based on Trinomial Distribution. *Journal of Applied Mathematics and Computation*, 7(2), 224-233.
DOI: 10.26855/jamc.2023.06.003

Received: May 28, 2023
Accepted: June 25, 2023
Published: July 21, 2023

***Corresponding author:** Mengke Ren, School of Mathematics and Physics, China University of Geosciences, Wuhan, Hubei, China.

Abstract

Infectious disease can be transmitted either through some fixed contacts or through some casual contacts. As the prevention and control measures (like contact restrictions and lock-downs) of an infectious disease change, the contact behavior among people may change. In this paper, by introducing a locality parameter, we consider the classical SIR model with two types of contacts: local contacts (individuals only contact their nearest neighbours on the lattice) and global contacts (individuals contact some other unknown people by chance). Then, we adopt the pair approximation approach to get a deterministic mean-field SIR model on square lattice by assuming that the distribution for errors (comparing with the expected value of the number of neighbours in a given state) follows trinomial. We calculate the basic reproduction number of the model, and establish the local stability of the disease-free equilibrium. In particular, three cases are focused: only global contact exists, only local contact exists, and both contacts exist. The existence and uniqueness of an endemic equilibrium in the first two cases, and the local stability of endemic equilibrium when only global contact exists are analyzed. Numerical simulations are performed to explore the effect of different interactions on the transmission dynamics.

Keywords

Pair-wise SIR model, Trinomial distribution, Basic reproduction number, Stability, Numerical simulations

1. Introduction

Epidemiology is a subject that studies the patterns of health and illness and associated factors at the population level [1]. Since the outbreak of COVID-19, the Chinese government has taken some measures to control the spread of the disease, such as “home office”, virus detection and quarantine, which has achieved good results [2-5]. For conventional spaces without prevention and control measures, people are in random contacts with others. However, the contact structure of the space may change under “home office” or other control measures [6-7]. Mathematical modeling of diseases is one of the effective methods for disease control and predictions [8].

Usually, compartmental models are proposed to describe the transmission dynamics of diseases, beginning with works by Kermack-McKendrick [9]. One of the classical models is the usage of Susceptible-Infectious-Recovered (SIR) epidemic model, which assumes a homogeneous population and constant infection and recovery rates. The approach by using network theory has become a major trend in modeling infectious disease [10-12], which is closer to the real transmission process. In fact, many infectious diseases actually spread through mutual contacts between individuals, which can be abstracted to complex networks for study [13-14]. One of the simplest network models is regular network, that is, each

node has the same number of potential contacts. Research methods on regular networks are divided into two types: cellular automata (CA) method and pair approximation (PA) method [15].

To address epidemic dynamics over regular or lattice-based networks, some researchers have considered a pair of nodes as basic variables to build pair-wise models. In a previous work, Keeling [16] considered a pair-wise SIR model having only local spatial structure on regular networks and proposed a pair approximation method to capture dynamic correlations between individuals using a closed system of ordinary differential equations. Inspired by the construction of small-world network, Maltz and Fabricius [17] proposed a deterministic approximation to the stochastic SIR model with the local and global contacts, where the local contacts on the square lattice are described by a pair approximation method. A locality parameter p is introduced to characterize the weight of global random contacts relative to local contacts. By adjusting p, this type of models have contact properties that interpolate between lattice-based (local) and mean-field based (global) contacts.

In the present work, we study a deterministic SIR model with local and global contacts based on the model proposed by Maltz and Fabricius[17], in which a stochastic SIR model with local and global contacts is also described. Based on existing models [18], Götz [19] analyzed the equilibria of the model in dependence of the locality parameter and the transmission rate of the disease and derived an explicit expression for the basic reproduction number in terms of the locality parameter and the disease parameters. A Poission distribution for the errors is used to derive the deterministic SIR model [17], but the impact of introducing different distribution for the errors of local contacts in such a model remains unexplored. In this work, our aim is to determine how a different distribution for the errors of local contacts alters the dynamics of an extended SIR epidemic.

2. Preliminaries

We consider the deterministic SIR model with local and global contacts formulated by Maltz and Fabricius [17]. All individuals are distributed on a two-dimensional $L\times L$ square lattice under periodic boundary conditions. The total number of nodes is $N=L^2$, and every node is in one of the three states: s (susceptible), i (infectious), and r (recovered). In addition, each one of the connected pairs is in one of the six states: ss, si, sr, ii, ir, rr. Infections occur through infectious contacts among susceptible and infectious individuals, and an infective contact is defined as a contact between two connected individuals such that if one individual is susceptible and the other infectious, the former becomes infectious. In the following, we first introduce the relationship between the number of nodes and connected pairs normalized by the total number of nodes.

2.1 Quantitative relationship

Assuming that the total number of nodes is normalized, i.e., $N=1$. Let $[m]$ be the number of nodes in state m normalized by the total number of nodes, $[mn]$ is the number of connected pairs in state mn, i.e., one node is in state m, while the other connected node is in state n, normalized by the total number of nodes. Then, the following relationship between the number of nodes and connected pairs (functions of the time t) normalized by the total number of nodes is obtained

$$[s]+[i]+[r]=1, \tag{1}$$

$$[ss]+[si]+[sr]+[ii]+[ir]+[rr]=2, \tag{2}$$

$$[s]=\frac{2[ss]+[si]+[sr]}{4}, \tag{3}$$

$$[i]=\frac{2[ii]+[si]+[ir]}{4}. \tag{4}$$

2.2 Parameters' definition and assumptions

The dynamics of the model can be described by a stochastic Markovian process, i.e., the state of node change is in one of the following processes: $s\to i$, $i\to r$, $s\to s$, $i\to s$, $r\to s$, and the last three processes denote birth and death. We define the transmission rate is β. Assume the weight of global causal contacts relative to local fixed contacts is p. The model is based on the following two assumptions.

A1: A node at a particular site has infectious contact with a randomly selected node on the lattice with transition rate

$p\beta$, and with one of its four nearest neighbors with the constant rate $(1-p)\beta$.

A2: Death is independent of node (individual) status. All newborns are susceptible, and an individual dies while at the same time an individual is born in order to avoid empty sites on the lattice. The birth and death rates are denoted as μ, and the recovery rate is defined by γ.

2.3 Deterministic approximation under trinomial distribution

To obtain a closed form of deterministic model, a pair approximation scheme is needed [16]. We consider the approximation when the errors in the closed system of equations follows a trinomial distribution. Let X_mX_n, X_nX_k be two different connected pairs with a common neighbor b, and the probability of reaching a given state (X_m state is m, X_n state is n and X_k state is k) at time t is approximated as

$$p_t(X_m \sim m, X_n \sim n, X_k \sim k) \approx \frac{<k>-1}{<k>} \frac{p_t(X_m \sim m, X_n \sim n)\, p_t(X_n \sim n, X_k \sim k)}{p_t(X_n \sim n)},$$

where $\langle k \rangle$ is the mean degree of a network.

Consider a square lattice, the mean degree the network is $<k>=4$, it follows that

$$p_t(X_m \sim m, X_n \sim n, X_k \sim k) \approx \frac{3p_t(X_m \sim m, X_n \sim n)\, p_t(X_n \sim n, X_k \sim k)}{4p_t(X_n \sim n)}.$$

Then, we use the above approximation scheme to deal with local contacts. To be specific, consider the correspondence between the "proportion" and the "probability": $[s]$ (the proportion of susceptible nodes) at time t can be considered as $p_t(X_m \sim s)$ (the probability that a given node is the type s node); $[si]/2$ (the proportion of node pairs) at time t can be considered as $p_t(X_mX_n \sim si)$ (the probability that a given node pair is the type si). Birth and death events are independent of the local structure.

For each process ($s \to i$, $ss \to si$, $si \to ii$, $sr \to ir$), we define the transfer rates r_1 and r_2 for local and global infections, respectively, and take the transfer rate $r =: qr_1 + pr_2$, $q = 1-p$.

For global contacts, $r_2 = \beta[i]$.

For local contacts, let ab be a pair of type si at a fixed time t. The infection transfer rate of node pair ab is the product of "β" and "the probability that the node's four nearest neighbors are infected nodes". Then r_1 can be regarded as $\beta(1+3p_1)/4$, where p_1 is the probability that a fixed triplet $X_mX_nX_k$ (X_k is a fixed nearest neighbor of X_n different from X_m) is in state ($X_m \sim i, X_n \sim s, X_k \sim i$), given that($X_m \sim i$, $X_n \sim s$). We conclude

$$p_1 = \frac{p_t(X_m \sim i, X_n \sim s, X_k \sim i)}{p_t(X_m \sim i, X_n \sim s)}.$$

Applying the previous approximation leads to

$$p_1 = \frac{3p_t(X_n \sim s, X_k \sim i)}{4p_t(X_n \sim s)}.$$

Following the correspondence between the "proportion" and the "probability", p_1 corresponds to $3[si]/16[s]$. Therefore, we have

$$r_1 = \beta\left(\frac{1}{4} + \frac{9[si]}{64[s]}\right).$$

3. SIR pair-wise model

Combining the previous preparations, we get the following SIR model with local and global contacts ($0 \le p \le 1$):

$$[\dot{s}] = -p\beta[s][i] - \frac{q\beta[si]}{4} + \mu[i] + \mu[r], \tag{5}$$

$$[\dot{i}] = -(\gamma+\mu)[i] + p\beta[s][i] + \frac{q\beta[si]}{4}, \tag{6}$$

$$[\dot{r}] = -\mu[r] + \gamma[i], \tag{7}$$

$$[\dot{ss}] = -2p\beta[i][ss] - \frac{9q\beta[si][ss]}{32[s]} + \mu[si] + \mu[sr], \tag{8}$$

$$[\dot{si}] = -p\beta[i][si] - q\beta\left(\frac{9[si]^2}{64[s]} + \frac{[si]}{4}\right) - (\gamma+\mu)[si] + 2\mu[ii] + \mu[ir] + 2p\beta[i][ss] + \frac{9q\beta[si][ss]}{32[s]}, \tag{9}$$

$$[\dot{sr}] = -p\beta[i][sr] - \frac{9q\beta[si][sr]}{64[s]} - \mu[sr] + \gamma[si] + \mu[ir] + 2\mu[rr], \tag{10}$$

$$[\dot{ii}] = -2(\mu+\gamma)[ii] + p\beta[i][si] + q\beta\left(\frac{9[si]^2}{64[s]} + \frac{[si]}{4}\right), \tag{11}$$

$$[\dot{ir}] = -2\mu[ir] - \gamma[ir] + 2\gamma[ii] + p\beta[i][sr] + \frac{9q\beta[si][sr]}{64[s]}, \tag{12}$$

$$[\dot{rr}] = -2\mu[rr] + \gamma[ir]. \tag{13}$$

In order to analyze the dynamics of this model, Eqs. (5)-(13) are simplified with the relationship between nodes and connected pairs. We mainly consider the following three cases.

3.1 Case 1: only global contacts

First, we consider the case of only global contacts existing ($p = 1$), that is,

$$[\dot{s}] = -\beta[s][i] - \mu[s] + \mu, \tag{14}$$

$$[\dot{i}] = -(\gamma+\mu)[i] + \beta[s][i], \tag{15}$$

$$[\dot{ss}] = -2\beta[i][ss] + 4\mu[s] - 2\mu[ss], \tag{16}$$

$$[\dot{si}] = -\beta[i][si] + 2\beta[i][ss] - (\gamma+2\mu)[si] + 4\mu[i]. \tag{17}$$

3.2 Case 2: only local contacts

Second, we consider the case of only global contacts existing ($p = 0$), that is,

$$[\dot{s}] = -\frac{\beta[si]}{4} - \mu[s] + \mu, \tag{18}$$

$$\dot{[i]} = -(\gamma+\mu)[i] + \frac{\beta[si]}{4}, \tag{19}$$

$$\dot{[ss]} = -\frac{9\beta[si][ss]}{32[s]} + 4\mu[s] - 2\mu[ss], \tag{20}$$

$$\dot{[si]} = -9\beta\left(\frac{[si]^2}{64[s]} - \frac{[si][ss]}{32[s]}\right) - \left(\frac{\beta}{4} + \gamma + 2\mu\right)[si] + 4\mu[i]. \tag{21}$$

3.3 Case 3: both contacts

For general case, when both contacts exist ($0 < p < 1$), we have

$$\dot{[s]} = -p\beta[s][i] - \frac{q\beta[si]}{4} - \mu[s] + \mu, \tag{22}$$

$$\dot{[i]} = -(\gamma+\mu)[i] + p\beta[si] + \frac{q\beta[si]}{4}, \tag{23}$$

$$\dot{[ss]} = -2p\beta[i][ss] - \frac{9q\beta[si][ss]}{32[s]} + 4\mu[s] - 2\mu[ss], \tag{24}$$

$$\dot{[si]} = -p\beta[i][si] - 9q\beta\left(\frac{[si]^2}{64[s]} - \frac{[si][ss]}{32[s]}\right) + 2p\beta[i][ss] - \left(\frac{q\beta}{4} + \gamma + 2\mu\right)[si] + 4\mu[i]. \tag{25}$$

4. Endemic equilibrium and stability

In this section, we analyze the equilibria and stability of the above models. Let $a = [s]$, $b = [i]$, $c = [ss]$, $d = [si]$. The model reaches stationary state, i.e., $\left(\dot{[s]}, \dot{[i]}, \dot{[ss]}, \dot{[si]}\right) = 0$.

From (22) - (24), we obtain

$$b = b(a) = \frac{\mu}{\gamma+\mu}(1-a). \quad d = d(a) = \frac{4}{q\beta}\mu(1-a)\left(1 - \frac{p\beta}{\gamma+\mu}a\right), \quad c(a) = \frac{32a^2}{9 + 7a + \frac{7p\beta}{\gamma+\mu}a(1-a)}.$$

From (25), we solve for a and get

$$U(a) = p\beta b(2c-d) + \frac{9q\beta(2c-d)}{64a}d - \left(\frac{q\beta}{4} + \gamma\right)d + \mu(4b-2d).$$

Since $U(a)$ contains $\mu(1-a)$, we take

$$U(a) \coloneqq \mu(1-a)\cdot W(a).$$

When $a = 1$, the disease-free equilibrium exists, i.e., $\xi = (1,0,2,0)$. The remaining equilibrium be zeros of the function $W(a)$.

4.1 Case 1: $p = 1$

When $p = 1$, the case corresponds to the classical SIR model, we have

$$U_1(a) = \mu(1-a)\left[1 - \frac{\beta a}{\gamma+\mu}\right], \quad W_1(a) = 1 - \frac{\beta a}{\gamma+\mu}.$$

Let $W_1 = 0$, we have $a_1^* = (\gamma+\mu)/\beta, b_1^* = \mu/(\gamma+\mu) - \mu/\beta$, $b_1^* > 0$. For $\beta > \gamma+\mu$, an endemic equilibrium exists, i.e.,

$$\xi_1^* = (a_1^*, b_1^*, c_1^*, d_1^*) = \left(\frac{\gamma+\mu}{\beta}, \frac{\mu}{\gamma+\mu}, -\frac{\mu}{\beta}, \frac{2(\gamma+\mu)^2}{\beta^2}, \frac{4\mu(\beta-\gamma-\mu)}{\beta^2}\right).$$

Theorem 1. If $p = 1$, i.e., only global contacts exist, the endemic equilibrium ξ_1^* is locally asymptotical stable.

Proof. When $p = 1$, let $\left([\dot{s}], [\dot{i}], [\dot{ss}], [\dot{si}]\right) = 0$.

Since $\xi_1^* = \left(\frac{\gamma+\mu}{\beta}, \frac{\mu}{\gamma+\mu}, -\frac{\mu}{\beta}, \frac{2(\gamma+\mu)^2}{\beta^2}, \frac{4\mu(\beta-\gamma-\mu)}{\beta^2}\right)$, from (14)-(17), the Jacobian matrix around the equilibrium ξ_1^* is

$$J^* = \begin{pmatrix} -\frac{\mu\beta}{\gamma+\mu} & -(\gamma+\mu) & 0 & 0 \\ \frac{\mu\beta}{\gamma+\mu} - \mu & 0 & 0 & 0 \\ 4\mu & -\frac{4(\gamma+\mu)^2}{\beta} & -\frac{2\beta\mu}{\gamma+\mu} & 0 \\ 0 & 4\left(\frac{\mu(\gamma+\mu-\beta)+(\gamma+\mu)^2}{\beta} + \mu\right) & \frac{2\mu\beta}{\gamma+\mu} - 2\mu & -\frac{\mu\beta}{\gamma+\mu} - (\gamma+\mu) \end{pmatrix}.$$

The trace of this matrix is negative, i.e.,

$$TrJ^* = -4\mu\beta/(\gamma+\mu) - (\gamma+\mu) < 0.$$

And the determinant is given by

$$DetJ^* = |J^*| = 2\mu\beta/(\gamma+\mu)\left(\mu\beta/(\gamma+\mu) + \gamma + \mu\right)\left(\mu\beta - \mu(\gamma+\mu)\right).$$

For $\beta > \gamma+\mu$, the equilibrium ξ_1^* exists, then $DetJ^* > 0$.

Hence the endemic equilibrium ξ_1^* is locally asymptotically stable if $\beta > \gamma+\mu$. □

4.2 Case 2: $p = 0$

From (18)-(21), we obtain the following equations:

$$b = \frac{\mu}{\gamma+\mu}(1-a), \quad c_0(a) = \frac{32a^2}{9+7a}, \quad d_0(a) = \frac{4}{\beta}\mu(1-a),$$

and

$$U_0(a) = \frac{9\beta(2c-d)}{64a}d - \left(\frac{\beta}{4} + \gamma\right)d + \mu(4b-2d).$$

Extracting a factor $\mu(1-a)$, we have

$$W_0(a) = \frac{4a}{9+7a} - \frac{\mu}{4\beta a} + w_0,$$

where

$$w_0 = \frac{4\mu}{\gamma+\mu} - \frac{16\gamma+31\mu}{4\beta} - 1.$$

To analyze the existence of roots, we expand the quadratic polynomial $W_0(a)$ by $a(9+7a)$, i.e.,

$$Y_0(a)=a(9+7a)\cdot W_0(a)=(4+7w_0)a^2+\left(9w_0-\frac{7\mu}{4\beta}\right)a-\frac{9\mu}{4\beta}.$$

Let $Y_0(a)=0$. Since $Y_0(0)=-9\mu/4\beta<0$, $Y_0(1)=16w_0+4-4\mu/\beta$, the roots of the above equation determine the existence and uniqueness of endemic equilibrium. For $4+7w_0>0$, i.e., $\beta>\beta_1=\frac{7(16\gamma+3\mu)(\gamma+\mu)}{100\mu-12\gamma}$, there exists a unique root $a_0^*>0$ given by

$$a_0^*=\frac{1}{2(4+7w_0)}\left(\frac{7\mu}{4\beta}-9w_0+\sqrt{\left(9w_0-\frac{7\mu}{4\beta}\right)^2+\frac{9\mu}{\beta}(4+7w_0)}\right).$$

We fixed $\gamma=1$ and $\mu=1$. From figure 1, only if the transmission parameter β is large enough there can exist a root $a_0^*\in(0,1)$. For $\beta=12$ (red solid) and $\beta=13$ (red dashed curve), there exists no root (equilibrium) $a_0^*<1$, while for $\beta=14$ (purple dashed curve) the endemic equilibrium $a_0^*\approx 0.9$ exists.

Hence, when $Y_0(a=1)>0$, i.e., $\beta>\beta^*=64\gamma+128\mu\Big/4\left(\frac{16\mu}{\gamma+\mu}-3\right)$, there exists a unique endemic equilibrium $a_0^*\in(0,1)$.

To sum up, when $\beta>\beta^*$, there exists a unique endemic equilibrium ξ_0^*, i.e.,

$$\xi_0^*=(a_0^*,b_0^*,c_0^*,d_0^*)=\left(a_0^*,\frac{\gamma}{\gamma+\mu}(1-a_0^*),\frac{32a_0^{*2}}{9+7a_0^*},\frac{4\mu}{\beta}(1-a_0^*)\right).$$

Therefore, it is shown that the disease-free equilibrium exists for all three cases. The endemic equilibrium exists and is unique for case 1 and case 2. And the endemic equilibrium is locally asymptotical stable for case 1.

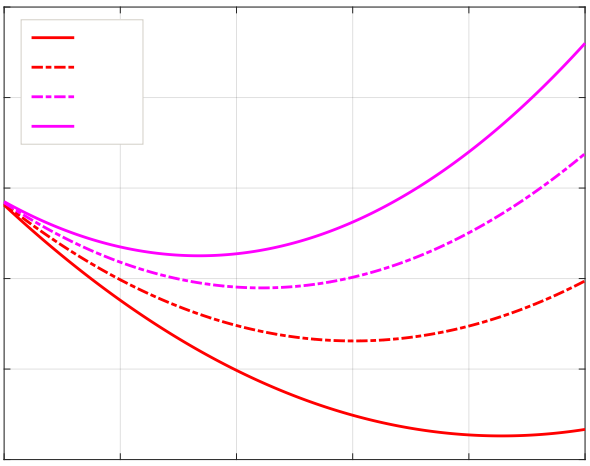

Figure 1. Plot of $Y_0(a)$.

5. Basic reproduction number

We use the next generation matrix approach to compute the basic reproduction number [20]. Noting that the disease-free equilibrium is $\xi=([s]^*,[i]^*,[ss]^*,[si]^*)=(1,0,0,2)$ for case 3.

First, we write the model for case 3 as (infected compartments x_i and non-infected compartments y_j),

$$x_i = \left([i],[si]\right), i = 1,2\,,\quad y_j = \left([s],[ss]\right), j = 1,2\,.$$

Thus, we divide the infected compartments into two parts,

$$x_i^{'} = \psi_i\left(x,y\right) - \upsilon_i\left(x,y\right),$$

where

$$\psi_i = \begin{pmatrix} p\beta x_1 y_1 + \dfrac{q\beta x_2}{4} \\ 2p\beta x_1 y_2 + \dfrac{9q\beta x_2 y_2}{32 y_1} \end{pmatrix}$$

and

$$\upsilon_i = \begin{pmatrix} \left(\gamma+\mu\right)x_1 \\ p\beta x_1 x_2 + \dfrac{q\beta}{4}x_2\left(\dfrac{9x_2}{16y_1}+1\right) + \left(\gamma+\mu\right)x_2 - \mu\left(4x_1 - x_2\right) \end{pmatrix}.$$

Then, linearizing the system around the disease-free equilibrium leads to the following matrices F and V as

$$F = \begin{pmatrix} p\beta & \dfrac{q\beta}{4} \\ 4p\beta & \dfrac{9q\beta}{16} \end{pmatrix},\quad V = \begin{pmatrix} \gamma+\mu & 0 \\ -4\mu & \dfrac{q\beta}{4}+\gamma+2\mu \end{pmatrix}.$$

Furthermore, the inverse of matrix V is

$$V^{-1} = \begin{pmatrix} \dfrac{1}{\gamma+\mu} & 0 \\ \dfrac{4\mu}{\left(\gamma+\mu\right)\left(\gamma+2\mu+\dfrac{q\beta}{4}\right)} & \dfrac{1}{\gamma+2\mu+\dfrac{q\beta}{4}} \end{pmatrix}.$$

Therefore, the next generation matrix is

$$K = FV^{-1} = \begin{pmatrix} p\beta & \dfrac{q\beta}{4} \\ 4p\beta & \dfrac{9q\beta}{16} \end{pmatrix}\begin{pmatrix} \dfrac{1}{\gamma+\mu} & 0 \\ \dfrac{4\mu}{\left(\gamma+\mu\right)\left(\gamma+2\mu+\dfrac{q\beta}{4}\right)} & \dfrac{1}{\gamma+2\mu+\dfrac{q\beta}{4}} \end{pmatrix} = \begin{pmatrix} pm_1 + \dfrac{q\mu m_1}{m_2} & \dfrac{q\beta}{4m_2} \\ 4pm_1 + \dfrac{9q\mu m_1}{4m_2} & \dfrac{9q\beta}{16m_2} \end{pmatrix},$$

where $m_1 = \dfrac{\beta}{\gamma+\mu}$, $m_2 = \gamma+2\mu+\dfrac{q\beta}{4}$.

Then the eigenvalues of K satisfy the following equation [20]

$$\lambda^2 - \frac{u+v}{16m_2}\lambda + \frac{w-l}{16m_2^{\,2}} = 0\,,$$

where $u = 16pm_1m_2$, $v = q\left(16\mu m_1 + 9\beta\right)$, $w = 9q^2\mu\beta m_1\left(m_2 - 1\right)$, $l = 7pq\beta m_1 m_2$.

Hence, for case 3, i.e., $0 < p < 1$, the basic reproduction number R_0 is given by

$$R_0 = \frac{1}{32m_2}\left(u+v+\sqrt{\left(u+v\right)^2 + 64\left(l-w\right)}\right).$$

For case 1, i.e., $p=1$, the basic reproduction number is simplified to

$$R_1 = m_1 = \frac{\beta}{\gamma+\mu}.$$

For case 2, i.e., $p=0$, the basic reproduction number is simplified to

$$R_2 = \frac{1}{32m_2}\left(16\mu m_1 + 9\beta + \sqrt{\left(16\mu m_1 + 9\beta\right)^2 - 576\mu\beta m_1\left(m_2 - 1\right)}\right).$$

Obviously [20], we have the following result.

Theorem 2. If $R_0 < 1$, the disease-free equilibrium is locally asymptotical stable, whereas if $R_0 > 1$, the disease-free equilibrium is unstable.

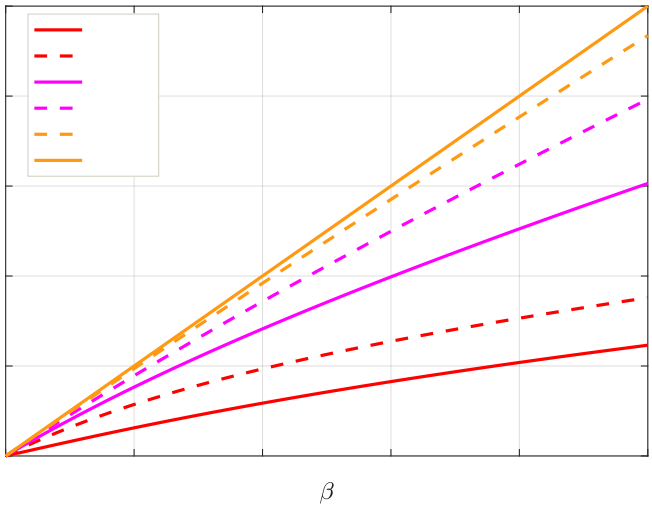

Figure 2. Plot of R_0 vs. β for $\gamma=1$, $\mu=1/2$ fixed.

6. Conclusions

In this paper, we consider the SIR model with global and local contacts under the assumption that the distribution for errors follows trinomial. The existence and uniqueness of the endemic equilibrium are discussed for case 1 (only global contact exists) and case 2 (only global contact exists), and the locally asymptotical stability of the endemic equilibrium is established for case 1. We use the next-generation matrix method to compute the basic reproduction number and analyze the local stability of the disease-free equilibrium for all three cases.

In order to investigate the influence of varying contact structures on the transmission process, we carry out the numerical simulations. By fixing the parameters $\gamma=1$ and $\mu=1$, we consider the influence of the transmission rate β on the basic reproduction number R_0 under different contact weights p. The simulation results (Figure 2) show that when the transmission rate β is fixed, the higher the contact weight p, the larger the basic reproduction number R_0. Combining with the COVID-19, measures such as short-term quarantine and home isolation are equivalent to reducing the contact weight p (global contact relative to the local contact), which can reduce the epidemic threshold and the risk of disease transmission. If some basic parameters of real-life infectious diseases are known, such as birth and death rates μ, recovery rates γ, and transmission rate β, we can use the model in this paper to predict the transmission thresholds of diseases under different contact structures. When the contact weight p reaches a certain threshold, the basic reproduction number R_0 will be equal to 1, and the disease reaches the epidemic threshold at this time. At this point, some measures such as home isolation can be taken to control the contact parameter p less than the critical value, then the disease epidemic can be controlled. Therefore, it is suggested that these measures could be properly taken to reduce the risk of disease transmission.

References

[1] Martcheva M. An introduction to mathematical epidemiology [M]. New York: Springer, 2015. DOI: 10.1007/978-1-4899-7612-3.

[2] Yamada T, Shi S. Estimating infection-related human mobility networks based on time series data of COVID-19 infection in Japan [J]. Applied Sciences, 2022, 12(18): 9236. DOI: 10.3390/app12189236.

[3] Ojo M M, Benson T O, Peter O J, et al. Nonlinear optimal control strategies for a mathematical model of COVID-19 and influenza co-infection [J]. Physica A, 2022, 607: 128173. DOI: 10.1016/j.physa.2022.128173.

[4] Martin L, Hauret L, Fuhrer C. Digitally transformed home office impacts on job satisfaction, job stress and job productivity. COVID-19 findings [J]. PLoS One, 2022, 17(3):e265131. DOI: 10.1371/journal.pone.0265131.

[5] Sánchez-Taltavull D, Castelo-Szekely V, Candinas D, et al. Modelling strategies to organize healthcare workforce during pandemics: Application to COVID-19 [J]. Journal of Theoretical Biology, 2021, 523:110718. DOI: 10.1016/j.jtbi.2021.110718.

[6] Costa C, Teodoro M, Mento C, et al. Work Performance, Mood and sleep alterations in home office workers during the COVID-19 Pandemic [J]. International Journal of Environmental Research and Public Health, 2022, 19(4):1990. DOI: 10.3390/ijerph19041990.

[7] Pfeifer M R. Human Resources during COVID-19: A monthly survey on mental health and working attitudes of Czech employees and managers during the year 2020 [J]. Sustainability, 2021, 13(18):10055. DOI: 10.3390/su131810055.

[8] Guimarães R M, Monteiro Da Silva J H C, Brusse G P D L, et al. Effect of physical distancing on Covid-19 incidence in Brazil: does the strictness of mandatory rules matter? [J]. Health Policy and Planning, 2021, 36(10):1605-1612. DOI: 10.1093/heapol/czab110.

[9] Kermack W O, McKendrick A G. A contribution to the mathematical theory of epidemics [J]. Proceedings of the Royal Society A, 1927, 115(772):700-721. DOI: 10.1098/rspa.1927.0118.

[10] Wang Y, Cao J, Huang G. Further dynamic analysis for a network sexually transmitted disease model with birth and death [J]. Applied Mathematics and Computation, 2019, 363:124635. DOI: 10.1016/j.amc.2019.124635.

[11] Bidari S, Chen X, Peters D, et al. Solvability of implicit final size equations for SIR epidemic models [J]. Mathematical Biosciences, 2016, 282:181-190. DOI: 10.1016/j.mbs.2016.10.012.

[12] Wren L, Best A. How local interactions impact the dynamics of an epidemic [J]. Bulletin of Mathematical Biology, 2021, 83(12):1-14. DOI: 10.1007/s11538-021-00961-w.

[13] Reijneveld J C, Ponten S C, Berendse H W, et al. The application of graph theoretical analysis to complex networks in the brain [J]. Clinical Neurophysiology, 2007, 118(11):2317-2331. DOI: 10.1016/j.clinph.2007.08.010.

[14] Bauch C T. The spread of infectious diseases in spatially structured populations: An invasory pair approximation [J]. Mathematical Biosciences, 2005, 198(2):217-237. DOI: 10.1016/j.mbs.2005.06.005.

[15] Sieburg H B, McCutchan J A, Clay O K, et al. Simulation of HIV infection in artificial immune systems [J]. Physica D, 1990, 45(1-3): 208-227. DOI: 10.1016/0167-2789(90)90184-Q.

[16] Keeling M J. The effects of local spatial structure on epidemiological invasions [J]. Proceedings of the Royal Society B, 1999, 266(1421):859-867. DOI: 10.1098/rspb.1999.0716.

[17] Maltz A, Fabricius G. SIR model with local and global infective contacts: A deterministic approach and applications [J]. Theoretical Population Biology, 2016, 112:70-79. DOI: 10.1016/j.tpb.2016.08.003.

[18] Dottori M, Fabricius G. SIR model on a dynamical network and the endemic state of an infectious disease [J]. Physica A, 2015, 434:25-35. DOI: 10.1016/j.physa.2015.04.007.

[19] Götz T. Analysis of an SIR--model with global and local infections [J]. arXiv preprint arXiv:2202.00322, 2022. DOI: 10.48550/arXiv.2202.00322.

[20] Van den Driessche P, Watmough J. Reproduction numbers and sub-threshold endemic equilibria for compartmental models of disease transmission [J]. Mathematical Biosciences, 2002, 180:29-48. DOI: 10.1016/S0025-5564(02)00108-6.